

AE 6042 A/Q Computational Fluid Dynamics

Final Project (Due Thursday, May 4, 2023)

Due Date Applies to Both Section A and Q Students

The objective for the final project is to develop a two-dimensional (2-D) finite-volume Euler/Navier-Stokes solver using your choice of methods, e.g., the Steger-Warming Flux Vector Splitting (FVS) scheme [1], Roe Flux Difference Splitting (FDS) scheme [2], or the Advection Upstream Splitting Method (AUSM⁺-up) FVS scheme [3]. The solver should be written using a high-order, Total Variation Diminishing (TVD), Monotone Upstream Scheme for Conservation Laws (MUSCL) formulation for the convective operator, and a second-order centered implementation of the diffusion operator. Develop the solver in two stages. First, establish a working implementation of the Euler equations starting with a first-order spatial formulation, then add the viscous diffusion operator to obtain the Navier-Stokes equations. The goal is to compute supersonic flow over the diamond shaped airfoil that was specified in Assignment 4 (see Fig. 1).

1. **Computational Domain:** The computational domain is shown in Fig. 1. The leading edge of the airfoil is placed at $(x, y) = (0, 0)$ and trailing edge at $(x, y) = (1, 0)$. The airfoil is symmetric in both coordinate directions. Its maximum half-thickness is located at $x = 0.5$ and is defined by two planar surfaces oriented at an angle of 10-degrees with respect to the leading and trailing edges (i.e. $y_{\text{half-thickness}} \approx 0.0882$). The symmetry lines at $y = 0$, upstream of the leading edge of the airfoil, and downstream of the trailing edge, are slipstreams that should be treated the same as adiabatic slip-wall conditions. For convenience, the upper wall boundary should also be treated using an adiabatic slip-wall condition. Inviscid adiabatic slip-wall conditions, viscous adiabatic no-slip wall conditions, and isothermal no-slip wall conditions will be successively applied to the airfoil surface, as specified below under the Project Tasks.

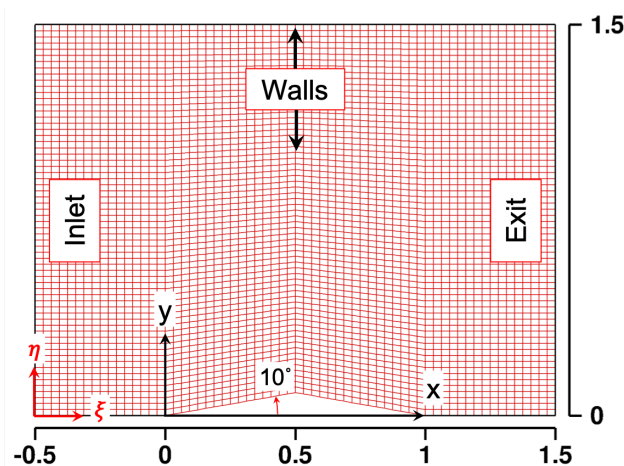


Figure 1. Computational domain and example grid for calculation of a supersonic flow over the top half of a diamond shaped airfoil in a channel. Assume that the spatial units are in meters.

2. **Grids:** Three primary grids are provided to use for this assignment, as shown in Fig. 2. Recall from Assignment 4 that grid points are described by Cartesian (x, y) coordinates at respective (i, j) locations, where the i index follows the ξ direction and the j index follows the η direction. Respective grids have integer dimensions of $n_x \times n_y$ over the ranges $1 \leq i \leq n_x$ and $1 \leq j \leq n_y$. Grid (a) has dimensions of 33×25 with uniformly spaced cells and should be used for developing and debugging the initial Euler solver. Grid (b) has dimensions of 65×49 with uniformly spaced cells and should be used to calculate the “production” level inviscid Euler cases specified below. Grid (c) has dimensions of 65×65 with stretching applied along the lower boundary to resolve the boundary layer associated with the no-slip wall conditions imposed for the viscous Navier-Stokes solutions. Coordinate data for each of these grids are provided in the ASCII formatted files “g33x25u.dat,” “g65x49u.dat,” and “g65x65s.dat,” respectively. The code that was developed to read and process the sample grid given in Assignment 4 (i.e., the “halo” (or “ghost”) cells, projected cell face areas, and cell volumes) should be used here as a starting point by adding the algorithmic details required for implementation of the Euler/Navier-Stokes solver.

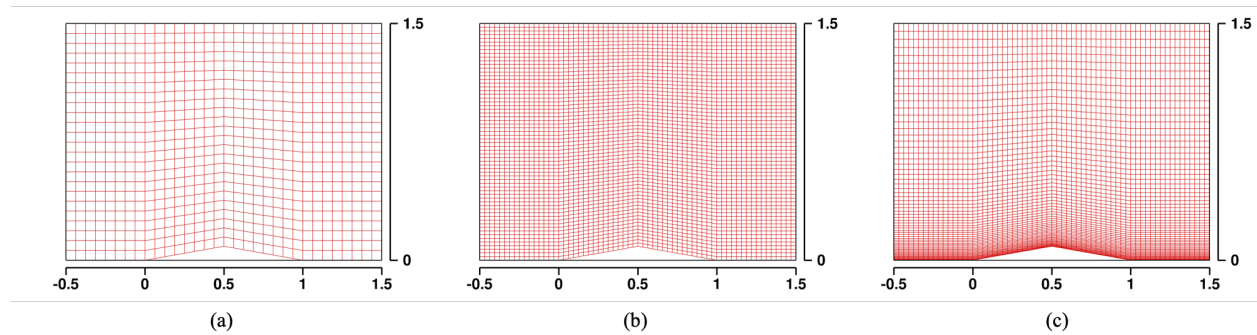


Figure 2. Primary grid topologies to be used for Euler and Navier-Stokes calculations with dimensions of (a) 33×25 uniformly spaced cells, (b) 65×49 uniformly spaced cells, and (c) 65×65 cells with stretching applied along the lower boundary to resolve the boundary layer associated with viscous no-slip walls. Coordinate data for each of these grids is provided in the ASCII formatted files “g33x25u.dat,” “g65x49u.dat,” and “g65x65s.dat,” respectively. **Assume that the spatial units are in meters.**

3. **Numerical Scheme:** The 2-D, time-dependent, Euler/Navier-Stokes equations should be solved using an *explicit* finite-volume discretization. Respective cell volumes and projected cell face areas must be evaluated for each cell in the computational domain. The equations will be marched forward in time until a steady-state solution is reached. To achieve this, first-order backward differencing in time should be combined with either the FVS or FDS schemes cited [1–3]. MUSCL interpolation/extrapolation should be used to approximate the left and right state vectors of $\mathbf{Q} = [\rho, \rho u, \rho v, \rho e_t]^T$ at respective cell faces.
4. **Thermodynamic and Transport Properties:** Assume that the working fluid is air at conditions where it behaves as a calorically perfect gas with an ideal gas constant of $\mathcal{R} = 287.0 \text{ J/(kg}\cdot\text{K)}$, constant pressure specific heat of $C_p = 1005 \text{ J/(kg}\cdot\text{K)}$, and ratio of specific heats of $\gamma = 1.400$. Use Sutherland’s formulas to calculate the viscosity and thermal conductivity in the diffusion operator (see Section 5.1.4 on page 333 in Anderson, Tannehill and Pletcher, 4th Edition).
5. **Initial and Boundary Conditions:** Assume that the static pressure, temperature, and Mach number at the inlet are 101325 Pa, 300.0 K, and $M = 2.000$, respectively, with a flow direction parallel to the Cartesian x -axis. This translates to an axial convective velocity of 694.4 m/s since the speed of sound for the conditions given is $c = 347.2 \text{ m/s}$. Using these conditions, the state vector \mathbf{Q} must be evaluated in all of the inlet boundary halos. Also use these values as the initial condition for all of the interior cells at the beginning of the calculation. This can be accomplished using the thermodynamic properties given above and recalling that

$$\rho e_t = \frac{p}{\gamma - 1} + \frac{1}{2} \rho (u^2 + v^2).$$

For the conditions given, the flow will be supersonic at both the inlet and exit planes. Thus, $\mathbf{Q}_{0,j}^{q+1} = \mathbf{Q}_{0,j}^q$ is held constant for all q along the inlet plane, and $\mathbf{Q}_{nx,j}^{q+1} = \mathbf{Q}_{nx-1,j}^q$ (i.e., first-order extrapolation) is applied along the exit plane after each iteration in time. Inviscid adiabatic slip-wall conditions should be applied along the upper wall and lower flow boundary on the intervals $-0.5 \leq x \leq 0.0$ and $1.0 \leq x \leq 1.5$. Adiabatic slip-wall conditions should be imposed along the surface of the airfoil over the interval $0.0 \leq x \leq 1.0$ for Euler calculations using Grids (a) and (b). No-slip adiabatic or isothermal conditions should be imposed for Navier-Stokes calculations using Grid (c), as specified below under the Project Tasks.

6. **Convergence Criteria:** Time marching methods for the solution of steady-state problems are a common strategy used in CFD. The governing system is cast in the form

$$\mathbf{Q}_{i,j}^{q+1} - \mathbf{Q}_{i,j}^q = -\Delta\tau \text{RHS}_{i,j}^q,$$

where the right-hand-side spatial operator is referred to as the residual since it approaches zero as the solution approaches a steady-state condition. This technique is known as “local-time-stepping,” and the time index q is typically used to denote iterations in “pseudo-time.” To drive the system to the steady-state solution, we are not concerned with time accuracy, but instead want to maximize the rate at which a given scheme converges to the steady-state solution. Thus, instead of applying a globally fixed time-step, which is required for a time-accurate calculation and produces variable CFL’s and VNN’s in the domain, these quantities can be fixed to their respective upper stability limits to maximize the local rate of convergence. The rate of convergence is typically characterized by the L_2 -Norm and/or L_∞ -Norm, where the L_2 -Norm is defined as

$$\|\mathbf{Q}_{i,j}^{q+1} - \mathbf{Q}_{i,j}^q\|_2 = \sqrt{\sum_{i=1}^{nx-1} \sum_{j=1}^{ny-1} |\mathbf{Q}_{i,j}^{q+1} - \mathbf{Q}_{i,j}^q|^2},$$

and the L_∞ -Norm is

$$\|\mathbf{Q}_{i,j}^{q+1} - \mathbf{Q}_{i,j}^q\|_\infty = \max_{i,j} \left\{ |\mathbf{Q}_{i,j}^{q+1} - \mathbf{Q}_{i,j}^q| \right\}, \text{ for } i = 1, 2, \dots, nx-1, \text{ and } j = 1, 2, \dots, ny-1.$$

Note that these quantities must be normalized by the relative magnitudes of the components of \mathbf{Q} . For this problem, normalization can be accomplished using the reference inflow pressure, temperature, and magnitude of velocity to define \mathbf{Q}_{ref} . The normalized quantities are plotted using \log_{10} values of the L_2 -Norm and L_∞ -Norm versus the number of iterations. Note that convergence to machine accuracy is 10^{-16} for codes compiled in double precision and 10^{-8} for codes compiled in single precision. For verification purposes, convergence to machine accuracy should always be demonstrated. In practice, reducing the slowest converging residuals by approximately 3 to 4 orders of magnitude is typically sufficient.

7. **Solution Verification:** The Euler solutions obtained with your solver should be verified by performing comparisons with the oblique shock solution given in Table 1. Oblique shock waves occur when a supersonic flow is forced to change direction (e.g., when it encounters the wedge). Thus, the given solution applies across the first oblique shock that forms at the leading edge of the airfoil.

Table 1. Weak oblique shock solution for $M_1 = 2.000$, turn angle of 10° , and $\gamma = 1.4$.

Wave Angle, degrees	M_2	p_2/p_1	ρ_2/ρ_1	T_2/T_1	p_{02}/p_{01}
39.31	1.641	1.707	1.458	1.170	0.9846

8. **Project Tasks:** Perform the following sequence of test cases to facilitate code development, debugging, and analysis of results:

- **Case 1:** Inviscid Euler, first-order accurate.
- **Case 2:** Inviscid Euler, second-order accurate (fully upwind) *or* third-order accurate QUICK scheme without flux limiter.
- **Case 3:** Inviscid Euler, second-order accurate (fully upwind) *or* third-order accurate QUICK scheme with basic minmod limiter.
- **Case 4:** Viscous Navier-Stokes, second-order accurate (fully upwind) *or* third-order accurate QUICK scheme with basic minmod limiter assuming the airfoil wall surface condition is adiabatic.
- **Case 5:** Viscous Navier-Stokes, second-order accurate (fully upwind) *or* third-order accurate QUICK scheme with basic minmod limiter assuming the airfoil wall surface condition is isothermal with $T_{\text{wall}} = 300.0 \text{ K}$.

Following the notation used in the Topic 25 class notes on pages 5 - 7, the spatial accuracy of the scheme can be set using the generalized interpolation stencils for the left and right states of \mathbf{Q} as follows: (1) first-order accuracy is obtained by setting $\epsilon = 0$, (2) second-order accuracy (fully upwind) is obtained by setting $\epsilon = 1$ and $\kappa = -1$, and (3) third-order accuracy using the QUICK scheme is obtained by setting $\epsilon = 1$ and $\kappa = 1/2$. Details related to the viscous diffusion operator are summarized in the Topic 4 class notes, and the 2-D operator in finite-volume form is summarized in the Topic 24 notes.

9. **Report:** Results should be documented in a neatly formatted typeset report with the following sections:

Cover Page

1. **Introduction (10 points)**
2. **Problem Formulation (20 points)**
3. **Results and Discussion (50 points)**
4. **Conclusions (10 points)**

Appendix (10 points): Computer code listing.

The main report (Sections 1 – 4) should be no longer than 15 single-sided pages (single-space, 11pt or 12pt font, 1-inch margins, not including the Cover Page and the Appendix). It should include all tables and figures discussed in your report and include at a minimum the following information:

- (a) A concise description of the numerical scheme used and how it was implemented.
- (b) Representative convergence plots for a subset of Cases 1 – 5 listed above (i.e., semi-log plots of the L_∞ or L_2 norm of the residual versus iteration number).
- (c) Results showing (for example) 2-D field plots of selected quantities of interest from Cases 1 – 5 (e.g., as listed in Table 1) combined with a discussion of the relative accuracy of the scheme's numerical predictions compared to the verification data given in Table 1.
- (d) An analysis and discussion that compares and contrasts the key differences observed between Cases 1 – 5. For example, the effects of higher-order accuracy with/without limiters compared to first-order accuracy, non-physical features such as the impact of numerical dissipation, differences between the inviscid and viscous flow solutions, and the effects of different wall boundary conditions.
- (e) A concise set of conclusions that summarizes the overall observations and trends observed.

A listing of your code should be provided in the Appendix along with a brief description of the computer architecture and compiler used to run the code. The program should be clearly written, commented, and be original work. **Identical codes submitted by multiple students will not be accepted.**

There is no advantage to handing in a long report. Covering the material described above clearly and concisely will yield maximum benefits. Given the page limits, you will need to present more than one neatly formatted table, diagram, or plot, etc., per page. Labels should be clearly legible using no smaller than a 10pt font size.

Please note the following. If difficulties are encountered in achieving a working version of the code or accomplishing the requested sequence of Project Tasks, the report should clearly outline the formulation, approach, progress made, difficulties encountered, and strategies pursued to overcome these difficulties.

Each student needs to write their own code and include a printout of the code as an appendix to the report. The code should be clearly commented and be original work. Plagiarizing or using a code written by someone else will be considered a violation of the Georgia Tech Honor Code.

Late reports cannot be accepted. Note that final grades for the class are due on Monday, May 8, 2023.

1 Bibliography

- [1] J. L. Steger and R. F. Warming. Flux vector splitting of the inviscid gasdynamic equations with application to finite-difference methods. *Journal of Computational Physics*, 40:263–293, 1981.
- [2] P. L. Roe. Approximate Riemann solvers, parameter vectors, and difference schemes. *Journal of Computational Physics*, 43:357–372, 1981.
- [3] M.-S. Liou. A sequel to AUSM, part II: AUSM⁺-up for all speeds. *Journal of Computational Physics*, 214:137–170, 2006.